Indonesian Journal of Electrical Engineering and Informatics (IJEEI)
Vol. 11, No. 4, December 2023, pp. 1038~1050
ISSN: 2089-3272, DOI: 10.52549/ijeei.v11i4.4836

Design and Realization of 2.4 GHz Bowtie Antenna for Ground Penetrating Radar (GPR)

Fatehi ALtalqi[1], Ulfa Elisa[2], Adil Echchelh[3]

[1,2,3]Department of Physics Laboratory of Electronics Treatment Information, Mechanic and Energetic, Faculty of Science of Kenitra, Ibn Tofail University, Morocco

Article Info

Article history:

Received May 31, 2023
Revised Nov 30, 2023
Accepted Dec 19, 2023

Keywords:

Design
Antennas
CST
Gain
GPR
Bandwidth
Bow-tie

ABSTRACT

In this research, a microstrip antenna with a bowtie hole was constructed. The proposed antenna is designed and fabricated to operate in the 2.4 GHz frequency band. Arc antennas are a popular choice due to their flat structure, lightweight design, wide bandwidth, and high gain characteristics for GPR applications. The antenna was designed as a microstrip antenna in the size of 58 mm x 69 mm. using an FR4 duplex printed circuit board with a material thickness of 1.6 mm, a dielectric constant of 4.3 and a transverse dielectric loss tangent of 0.02. The design and simulation were performed using CST Studio Suite programming. The results of the simulation and measurements antenna were tested for resonant frequency, return loss, VSWR, bandwidth, impedance, and polarization, and the simulation results were compared. The measurements carried out with a Vector Network Analyzer, showed a return loss of -18, a VSWR of 1.29, a bandwidth of 100 MHz, an impedance of 47 ohms, and a high gain of 18 dB at 2.42 GHz. Both the simulation and measurement results demonstrated good agreement, with frequency bands of interest that were very close and stable with high-gain omnidirectional radiation characteristics. Thus, the antenna is well-suited to meet the requirements of GPR applications.

Corresponding Author:

Fatehi ALtalqi
Department of Physics Laboratory of Electronics Treatment Information, Mechanic and Energetic, Faculty of Science of Kenitra, Ibn Tofail University, Morocco
fatehi.abdullah2009@gmail.com

1. INTRODUCTION

GPR systems prove to be efficient non-destructive instruments that employ the transmission and reception of electromagnetic waves for detecting targets beneath various surfaces[1]. It finds application in tasks such as characterizing tile breakages, conducting soil surveys, analyzing asphalt structures, and hole discovery in vulnerable areas [2]. In simple terms, ground-penetrating radar (GPR) has proven to be a valuable tool in diverse fields, including engineering, geophysics, archaeology, and more[3]. The capabilities of this radar are constrained by factors such as frequency, bandwidth, gain, and other parameters necessary for detecting the desired target, be it natural or man-made, in the presence of a complex medium[4].

The Ground Penetrating Radar (GPR) system comprises two antennas: one serves as the transmitting antenna, emitting electromagnetic waves, while the other serves as the receiving antenna, functioning either independently or simultaneously with the transmitting antenna[5]. Transmitting antennas produce electromagnetic waves, directing them towards objects buried in the ground or concealed behind walls [6]. The velocity of the wave aligns with the dielectric constant of the medium. Upon encountering an object, a portion of the wave is reflected by the object, and this reflected segment is captured by the receiving antenna. antennas play a crucial role in GPR systems, necessi-tating designs that fulfill specific system requirements. These include the capacity to operate at low frequencies for enhanced depth of penetration, as well as the ability to function at high frequencies to achieve superior resolution for discerning small targets[7]-[8]. Since the antenna is the most important component of ground penetrating radar, because the antenna's performance directly influences the imaging quality of the GPR system. Hence, the design and advancement of antennas are

imperative in enhancing the overall performance of GPR systems [9]- [10]. Ultra-wideband (UWB) technology can attain high-resolution imaging [11]. It is a widely recognized fact that subsurface lossy mediums lead to rapid decay of electromagnetic waves[12]. Therefore, antenna design must prioritize a low operating frequency to achieve adequate penetration depth. However, achieving a balance between low operating frequency, high gain, and wide bandwidth has posed a significant challenge in GPR antenna design [8]. GPR should meet specific measures to work effectively, which incorporate adequate signal-to-noise ratio, motion toward noise ratio (SNR), target accuracy, and target depth precision [13].

These antennas must be well-designed, considering the proximity of the framework to the ground [14].

Designers must consider various characteristics such as signal propagation mode, subsurface dielectric properties, frequency, and data transmission[15].

In a ground-penetrating radar (GPR) system, the operating frequency determines the depth of penetration, while the signal bandwidth affects the system's accuracy. The propagation medium is typically heterogeneous and lossy and better accuracy with high frequencies. The antenna should possess certain characteristics such as high gain [16] .

Accordingly, the types of receiving antennas that can meet these requirements are limited to dipole antennas, Vivaldi transverse electromagnetic horn (TEM) antennas, bowtie antennas, planar helical antennas, and arc antennas typically used in ground-penetrating radar (GPR) applications due to their various advantages. Bowtie antennas[17]. Antennas are particularly popular due to their uncomplicated structure and linear phase characteristics within the operating frequency range.This can be attributed to its favorable attributes, including high gain, relatively broad bandwidth, and straightforward manufacturing process [18].with their compact size and affordable price, have gained significant interest in various telecommunications applications [19] .They can be designed and manufactured for use in narrow and ultra-high bandwidth frequency bands, and microstrip antennas can be implemented in different sizes and configurations. Bowtie antennas have been widely used in wide-range radars due to their enhanced return loss, high gain, impedance, and radiation pattern stability [20]

In this study, a bowtie antenna was designed and simulated to create a bowtie antenna suitable for GPR applications[21]. The proposed antenna was designed and simulated using CST Microwave Studio v14 and then fabricated. The antenna was based on a tripod configuration and had a gain of 20 dB, a return loss of -25.49 dB, a VSWR of 1.12, and a bandwidth of 210 MHz. The impedance of the antenna was 47.04 Ω, and it exhibited an omnidirectional radiation pattern with a size of 58 mm × 69 mm. The dielectric constant (εr) was 4.3, and the dielectric loss tangent (tan δ) was 0.02. The simulation and measurement results demonstrated good characteristics and high gain for the bowtie antenna.

2. GROUND PENETRATING RADAR(GPR)

Ground Penetrating Radar (GPR).is a type of radar system used as a tool to detect and locate buried objects or structures beneath the Earth's surface or within objects that are not visible to the naked eye through the use of electromagnetic waves. Antennas play a crucial role in the ground-penetrating radar (GPR) systems, as they serve as the primary components that transmit and receive electromagnetic waves in the frequency range from MHz to GHz. The block diagram of a GPR system, illustrated in Figure 1, includes a transmitter that emits energy pulses into the ground via an antenna and a receiver that captures these pulses via another antenna. The signal is connected to the signal processing and is reflected by the object. After that, the processor processes the signal data to make it visible on the display screen. The GPR antenna is not supposed to be in contact with the Earth's surface, so it can take measurements quickly Understanding the diverse ground characteristics is paramount for effective GPR application. Soil composition, moisture content, and geological features significantly impact the radar signals' propagation and reflection. [22].

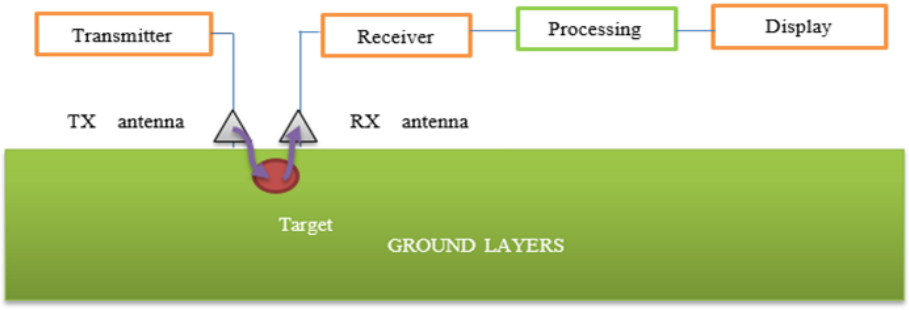

Figure 1. Ground Penetrating Radar (GPR)

3. RESEARCH METHOD

3.1. Microstrip Antenna Structure

The initial phase in the antenna design process entails employing the provided formula to compute the anten-na's dimensions [23]. Typically, a basic microstrip antenna comprises three layers: the patch layer, dielectric substrate, and ground planethese computations ascertain both the length and width of the antenna. The microstrip patch antennas are designed and simulated with an emphasis on meeting a frequency requirement of 2.4 GHz with using FR-4 substrate, characterized by a thickness of 0.0035 mm .The development process involves employing a substrate with a relative permittivity (εr) of 4.3, a loss tangent ($tan\ \delta$) of 0.02, and a thickness (h) of 1.6 mm [24]. Using copper annular in the ground plane and patch. When designing a microstrip antenna, various parameters must be considered, the thickness of the patch and ground, and the dimensions of the substrate in terms of width ,length of ground , substrate and patch and can be calculated using the provided equations [25].

$$W = \frac{\lambda_o}{2\sqrt{\frac{1}{2}(\varepsilon_r+1)}} \quad (1)$$

Calculating the effective dielectric constant, by using Equation (2)

$$\varepsilon_{eff} = \frac{\varepsilon_r+1}{2} + \frac{\varepsilon_r-1}{2}\left(\frac{1}{\sqrt{1+12\frac{h}{w}}}\right) \quad (2)$$

Calculating the length extension of the patch, by using the equation (3)

$$\triangle L = 0.412h\left[\frac{E_{reff+0.3}\left(\frac{w}{h}0.264\right)}{E_{reff}-0.258\left(\frac{w}{h}+0.8\right)}\right] \quad (3)$$

The actual length of the rectangular patch, L is calculated by the equation

$$L = L_{eff} - 2 \triangle L \quad (4)$$

Where L_{eff} is the effective length and is calculated.

$$Leff = \frac{c}{2f_0\sqrt{E_{eeff}}} \quad (5)$$

3.2. Bowtie Antenna Theory

In figure 2. This section details the design of the bowtie for antenna. The primary configuration of the slot triangular, defined by three boundaries, is outlined, highlighting the significance of the flare point "θ0" in determining bandwidth, the impact of hole distance "g" on antenna performance, and the close correlation between slot length "b" and slot width "a" with radiation efficiency. On the copper patch, the triangular slots on the right side are etched out and the left side. Approximate equations are employed to calculate the dimensions of these triangular-shaped bowtie slot [26] [27].

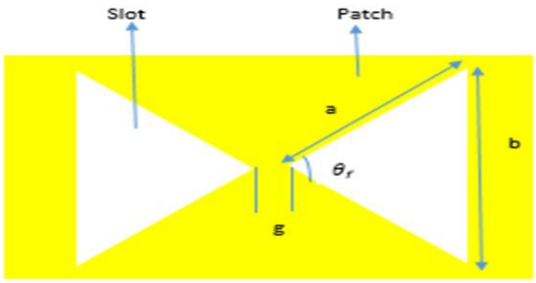

Figure 2. Basic geometry of triangular slot of The Bowtie [28]

The characteristic impedance of the bowtie antenna can be expressed as follows [29]

$$Z_c = 120 \ln\left(\cos\left(\frac{\theta o}{4}\right)\right) \quad (6)$$

Where θ0 is the flare angle. The length of the bowtie antenna can be determined using the following equation.

$$l = \lambda_0 \left(\frac{1}{\sqrt{\varepsilon ef}}\right) \quad (7)$$

Where λ0 is the wavelength, the effective relative permittivity of the antenna can be calculated using the following equation (3):

$$\epsilon eff = \left(\left(\frac{\epsilon r+1}{2}\right) + (\epsilon r - 1)\left(1 + \left(10\frac{h}{w}\right)\right)^{-0.555}\right. \quad (8)$$

Where w is bowtie antenna width, h a substrate thickness and ϵr is substrate constant dielectric. The frequency resonant corresponding to the various modes is given.
Where w and h are in mm. The resonant frequency (fr) of the different modes of the antenna by equation:

$$fr = c\frac{Kmn}{2\pi\sqrt{\epsilon r}} \quad (9)$$

Where fr is resonant frequency, Kmn of resonating modes, m, and n are the number of modes, and c is velocity of light in free space, we can be calculated. The side length and width of the bowtie antenna strip. Using equations, a and b [30]

$$a = \frac{1.6\lambda}{\sqrt{\epsilon_r}} \quad (10) \qquad \text{and } \lambda = \frac{c}{f} \quad (11)$$

$$b = \frac{0.5\lambda}{\sqrt{\epsilon_r}} \quad (12)$$

As for determining the size of a bowtie-shaped slot, equations 10 and 12.

3.3. CPW Feed Line Design

The configuration of the slot antenna fed by coplanar waveguide (CPW) is illustrated in Figure 1, detailing all relevant dimensions. This antenna features a CPW-fed triangular-ring slot The generation of linearly-polarized antenna radiation along the width of the bow-tie slot is achieved by activating two CPW apertures, each configured to present a 50 ohm impedance for compatibility with the measurement system. In this investigation, the choice of a coplanar waveguide feed line for the antenna is deliberate, driven by various factors. These include its controlled characteristic impedance, facile connection to a slightly scaled-down version of the antenna, and the comparatively broader bandwidth of the antenna.

The provided formulas are employed for calculations, with a parametric investigation involving the adjustment of specific parameters such as the microstrip line gap (g), slotted feedline gap (wf), and slotted feedline height (lf). The impedance (Z0) of the coplanar waveguide (CPW) line can be ascertained by applying the equations outlined [20]

$$Z_0 = \left(\frac{30x\pi}{\sqrt{\epsilon_{eff}}}\right)\left(\frac{K(k')}{K(k)}\right) \quad (13)$$

Where the effective dielectric constant of the substrate is given in equations.

$$\epsilon_{eff} = \{(\epsilon_r - 1)/2\}\left\{\left(\frac{K(k')}{K(k)}\right)\left(\frac{K(k_1)}{K(k_1')}\right)\right\} \quad (14)$$

$$k = \frac{w}{w+2s} \quad (15)$$

In addition, $k_1 = \frac{sinh\left(\frac{\pi w}{4h}\right)}{sinh\left(\frac{(w+2s)\pi}{4h}\right)}$ (16)

$$k' = \sqrt{1-k^2} \quad (17)$$

Figure 3 (a) . Front view depicts the bow tie antenna's design. The antenna is made of copper for patch and ground plane an FR-4 substrate. CPW line powers it. The copper covering has a thickness of tc = 0.035 mm. Several simulations in CST Microwave Studio were largely used to optimize the antenna dimensions in figure 3 (b) the parameters of final displayed in the table.1, figure 3(c) Design of a antenna in CST.

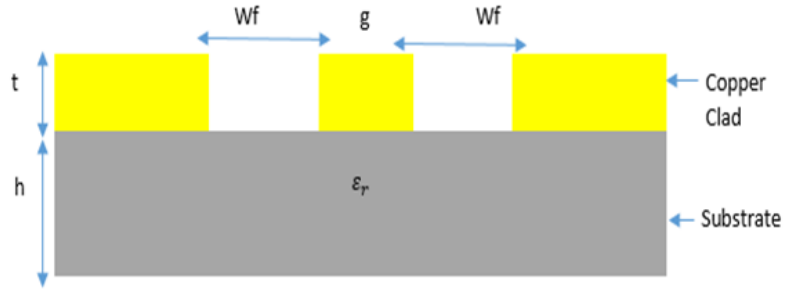

(a)

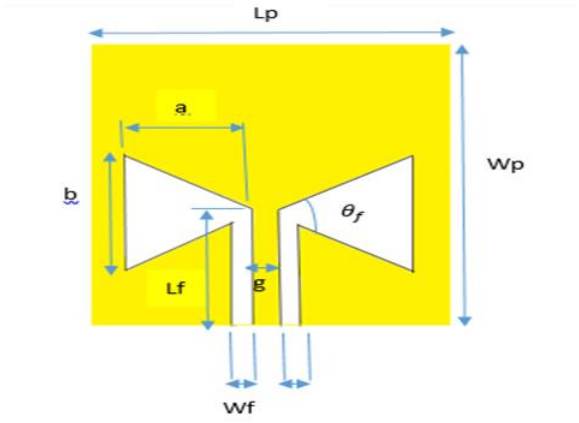

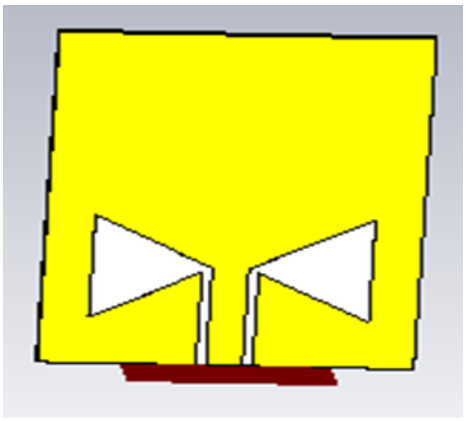

(b) (c)

Figure 3. Front view (a) Geometry of bowtie antenna Top view (b) Design of a antenna in CST (c)

Table 1. The proposed Design Parameters for Bowtie the Antenna

Parameters	Symbol	Values (mm)
The height of the conductor	ts	0.0035
The dielectric constant of substrate	ϵr	4.3
Slot Length	b	38
Slot Width	a	20.5
Length of feed	Lf	20
Gap strip width	g	5.7
Width of the substrate, FR4	Ws	58
Length of the substrate, FR4	Ls	69
The substrate height, FR4	h	1.6
Width of the ground	Wg	58
Length of the ground	Lg	7
Width of the patch	Wp	58
Length of the patch	Lp	69
Width of the feed line	Wf	3

4. RESULTS AND DISCUSSION

4.1. Simulation Result in CST Microwave Studio

In this section, the simulation results of the proposed bowtie antenna will be presented along with a clear and easy analysis of each result. The bowtie antenna simulation was conducted using CST Microwave Studio. In Figure 4, the reflection coefficient curve of the bowtie antenna simulation result is shown. It can be observed that the antenna operates at a frequency of 2.4 GHz. The return loss was -25.49 dB, and the antenna has a bandwidth of 210 MHz, ranging from 2.29 GHz to 2.50 GHz. Figure 5 shows the voltage standing wave ratio (VSWR), which indicates the amount of power reflected by the simulated antenna.

It is recommended for the VSWR value to be less than 2 and greater than or equal to 1, as a lower value indicates improved antenna performance. In Figure 5, the simulated VSWR value is 1.2 at 2.4 GHz, demonstrating the well-designed characteristics of the bowtie antenna. Figure 6 illustrates the impedance, which equals 47.04 ohms, for the bowtie antenna. Furthermore, Figure 7 displays the gain of the bowtie

antenna, which reaches 20 dB at its center frequency of 2.4 GHz. The antenna exhibits strong directional features and performs exceptionally well in terms of gain. As a result, this antenna is an excellent choice for ground-penetrating radar applications.

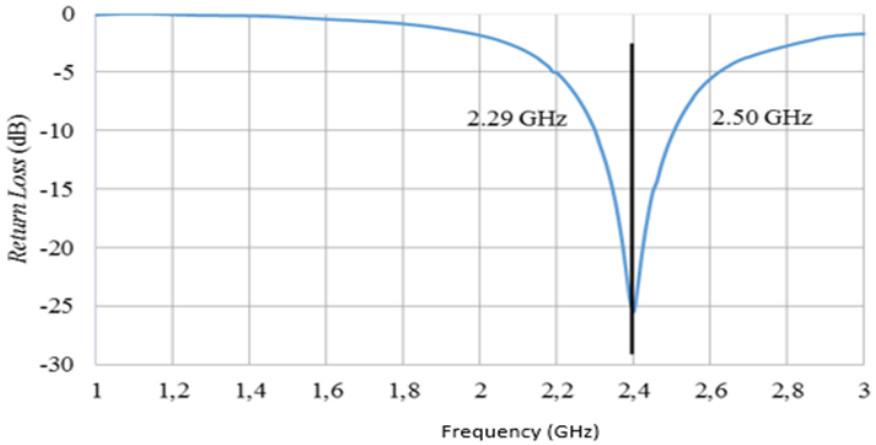

Figure 4. S-parameters of antenna

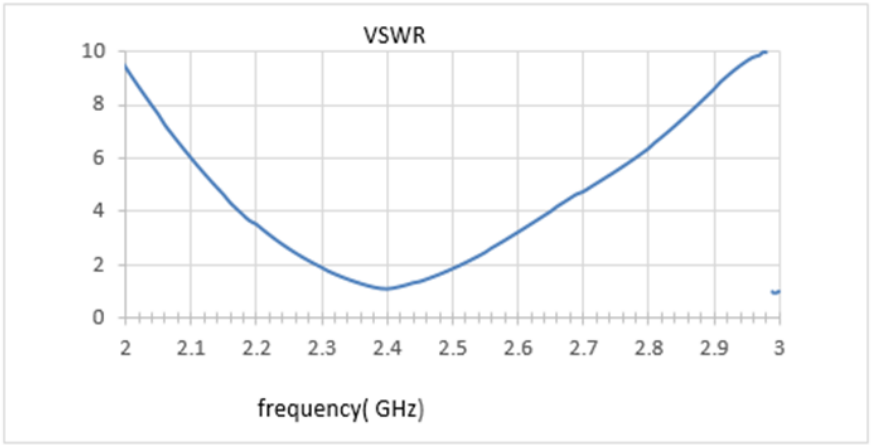

. Figure 5. VSWR of antenna

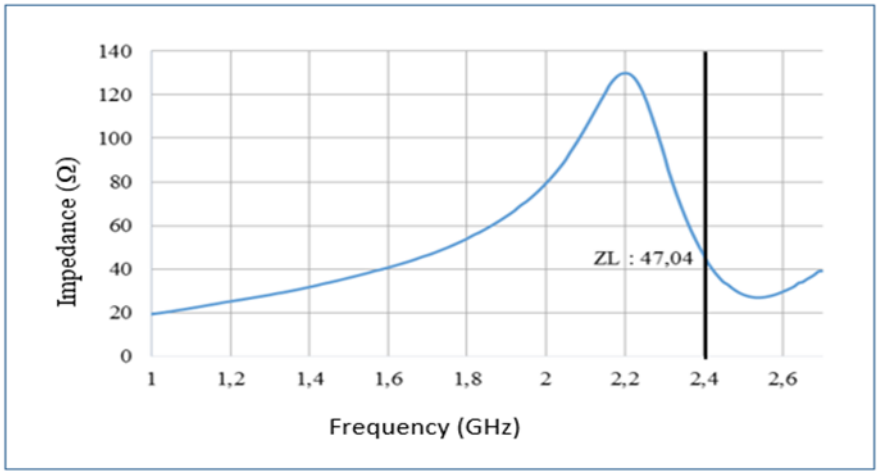

Figure 6. Impendence of antenna

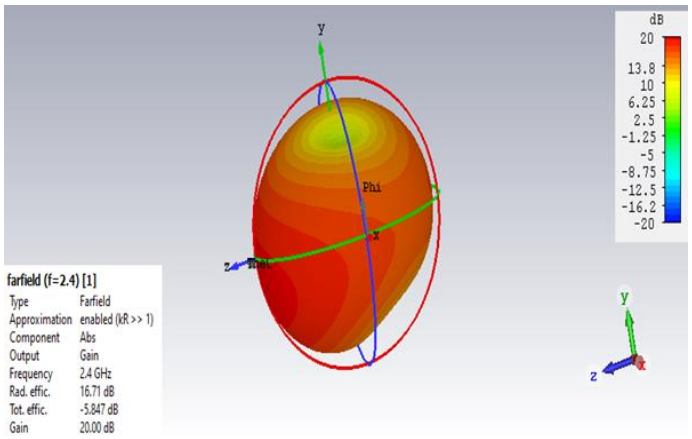

Figure 7. Gain 3D radiation pattern of Antenna

4.2. Fabrication and Measurement Environment

The antenna was fabricated using the Gerber files created by CST Microwave Studio and an automated computerized numerical control prototyping machines A437. It was used FR4 substrate material with a permittivity of 4.3. Board is cut to a size of 58 mm × 69 mm. The figure 8 shows a of he fabrication of the bowtie antenna. While the figure 9 illustrates the experimental configurations for S11, radiation patterns, and the corresponding measured environment. The S-parameter (S11) of the fabricated prototype was measured using a PNA Network Analyzer (Model: E5071C-4K5), which operates in the 300 KHz–20 GHz range. Radiation pattern measurements were performed in an anechoic chamber is depicted in figure 10.

Figure 8. Antenna After Fabrication

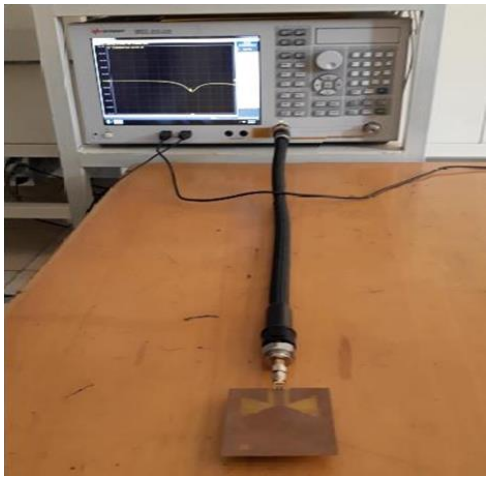

Figure 9. Antenna Measurements with a Vector Network Analyzer

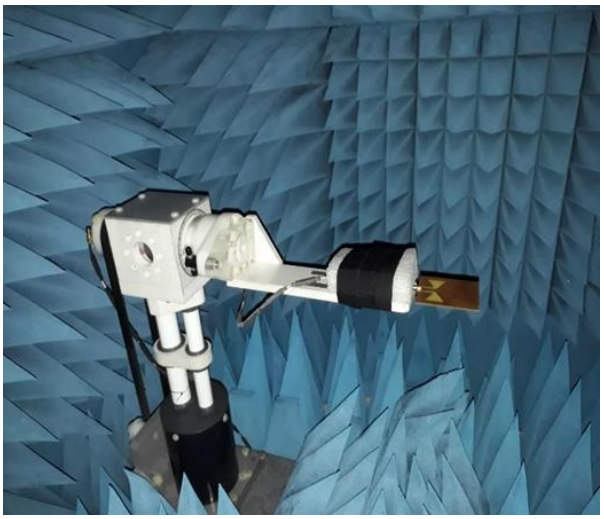

Figure 10. Antenna Measurements with Anechoic Chamber

4.3. Measurement Display on Vector Network Analyzer

The results of the Measurement for fabricated antenna were obtained through the utilization of the Vector Network Analyzer (VNA), as depicted in figures 11, 12, and 13.

In figure 11, the return loss (S- Parameter) is illustrated, revealing a peak value of -18 dB at 2.42 GHz, accompanied by an approximate bandwidth of 100 MHz. Furthermore, the figure 12 illustrates the VSWR plot for the fabricated antenna, showcasing a minimum value of 1.29 at the frequency of 2.19GHz, and the impendence of 40.99 ohm at 2.42GHz is depicted in figure 13.

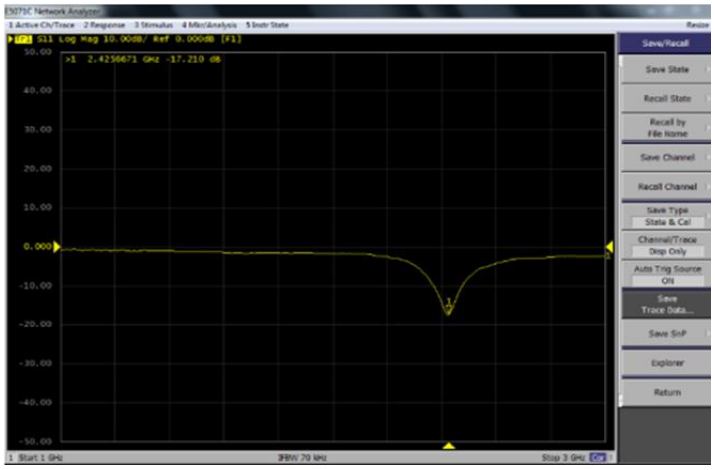

Figure 11. Return loss display

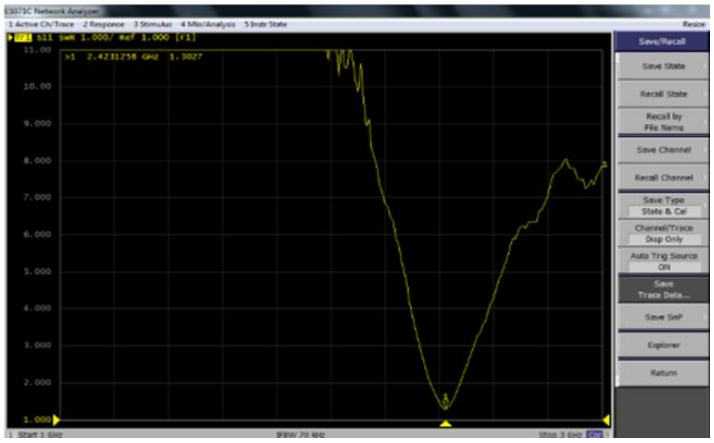

Figure 12. VSWR display

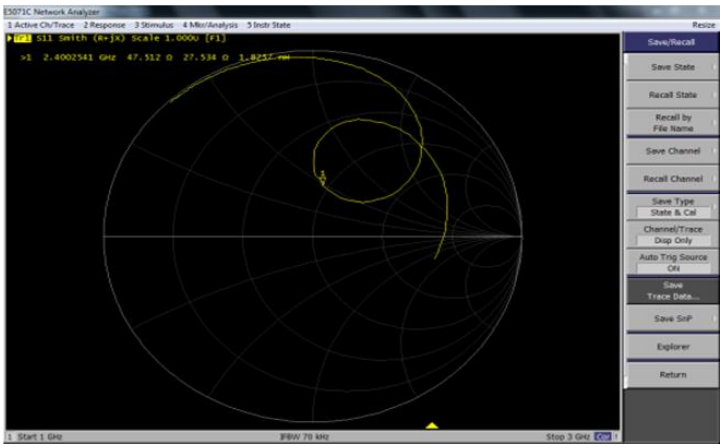

Figure 13. Input Impedance Display

4.4. Influence and comparative analysis of simulation and measurement results

Impact and comparative analysis of simulation and measurement results the measured antennas must have results similar to or close to the parameters of the designed antenna, and to obtain these parameters, it is observed that the antenna produces a value that does not differ significantly from the parameters of the designed antenna.

When measuring the antenna, the obtained frequency value is 2.42 GHz. This value is for the 2.4 GHz frequency band, which indicates that the design was good. In the following stages, the simulated and measured results are clarified and compared.

4.5. Comparison resuls of simulation and measurement

4.5.1 Return loss and bandwidth of the antenna across frequency

Figure 14 below shows a comparison between the simulated and measured The simulation results indicate a return loss value of -25.49 dB at 2.4GHz, while the measured results indicate a value of -18dB at 2.42 GHz. The simulation results indicate a bandwidth value of 210 MHz, while the measured results indicate a value of 100 GHz. Despite this difference, both the simulation and fabrication of the microstrip slot bowtie antenna have met the desired standards, as they can operate within the frequency range of " 2.4 GHz to 2.48 GHz".

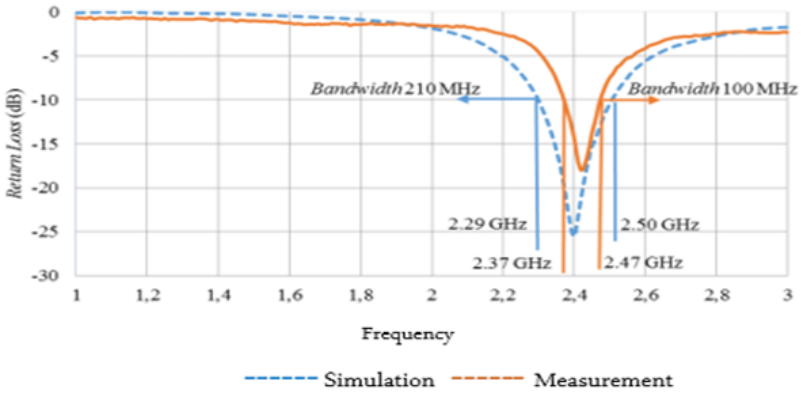

Figure 14. Simulated and Measure Return Loss and bandwidth

4.5.2 Impendence

The impedance is the ratio of the power present at the antenna terminals. Figure 15 is a comparison of the simulation results and measurement results.

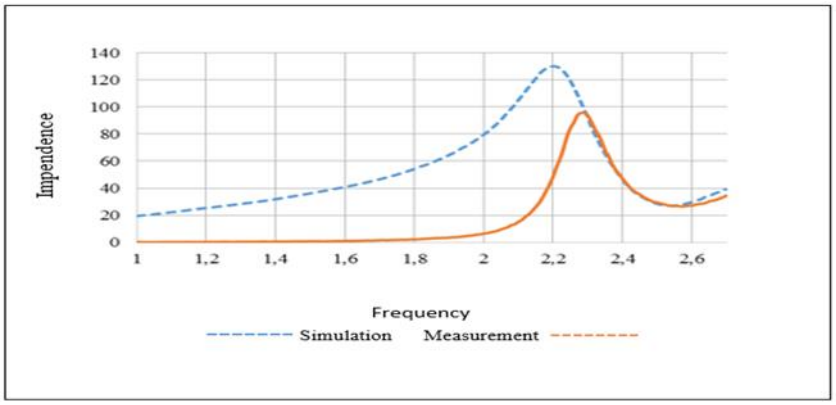

Figure 15. Simulation and Measurement Impendence

4.5.3 Standing Wave Ratio of Voltage (VSWR)

Based on figure 16. the value of VSWR obtained from the simulation results is 1.112 at a frequency of 2.4 GHz while the measurement results obtained a value of 1.292 at a frequency of 2.42 GHz. It can be seen that the simulation results are close to the measurement results, and this gives the impression that the design and fabrication of the antenna went through stages under good conditions.

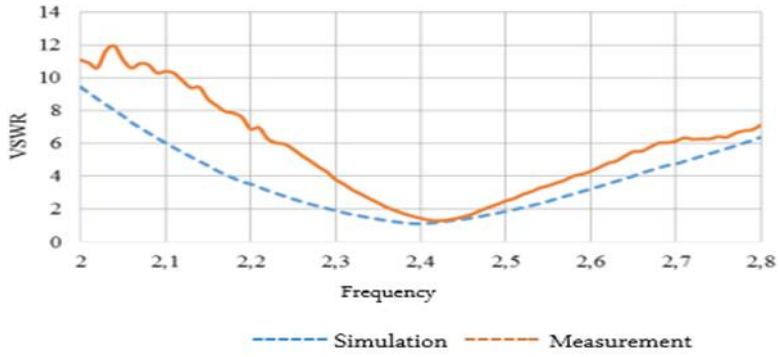

Figure 16. VSWR of a bow-tie antenna

4.5.4 Radiation Patterns

Radiation polarization measurements are performed to determine the direction of wave emission from the designed antenna. The measurement results using an anechoic chamber can be seen in Figure 17. It can be seen that the antenna polarization from simulation results and measurements is almost the same, that is omnidirectional and bidirectional. The radiation pattern measurements in both figures show that the simulated antenna's radiation pattern is similar to the measured antennae.

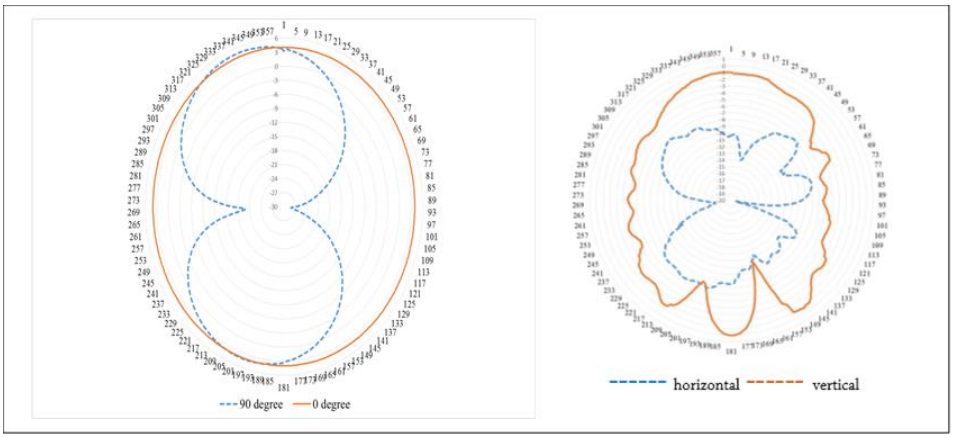

(a) (b)

Figure 17. 2D Radiation Pattern simulation (a) and Measurement (b)

4.5.5 The Gain

Figure 18 illustrates that the microstrip antenna within the necktie slot structure achieves a maximum gain of 18 dB at a frequency of 2.42 GHz. This gain value, as obtained from the measurements, is considered very excellent. The higher the gain obtained, the better the antenna's transmitting power will be.

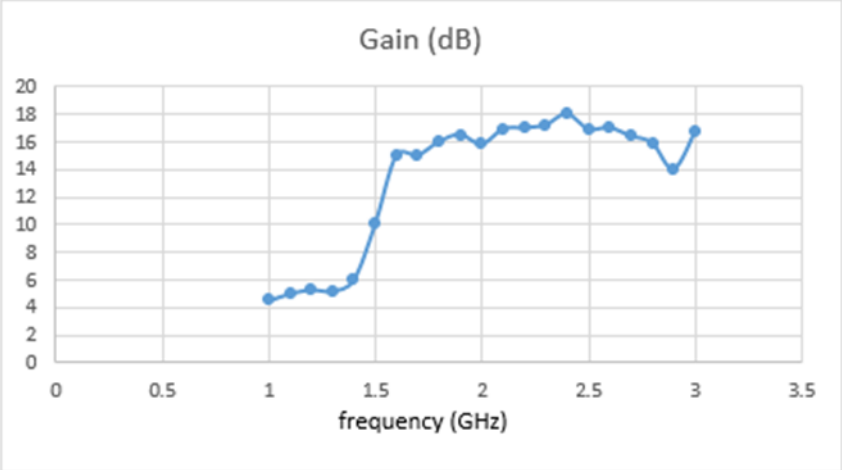

Figure 18. Measurements gain Results in 3D

Table 2 showcases comparison of the simulated and Measurements reseluts for the antenna fabricatedat the resonant frequency of 2.4 GHz. The comparison includes various parameters such as S-Parameter, bandwidth and VSWR, Radiation Pattern, impedance, gain

Table 2. Simulation and Measurement Results for Antenna Parameter

Antenna Parameter	Simulation	Measurement
Frequency (GHz)	2.4 GHz (2.29 – 2.50)	2.42 GHz (2.37 - 2.47)
Return Loss (dB)	-25.49	-18.00
Bandwidth (MHz)	210	100
VSWR	1.12	1.292
Radiation Pattern	Omnidirectional	Omnidirectional
Impedance (Ω)	47.04	40.99
Gain (dB)	20	18

In this investigation, the design put forth in this study underwent a comprehensive evaluation in comparison to other works highlighted in recent literature (enumerated in Table 3 [31], [32]) This comparative analysis primarily emphasized some parameters in assessing the performance of the antenna. Structure, Frequency, Gain, Ease of the fabrication

Table 3. compared antenna performance parameters with the previous refrences

Author	Structure	Frequency(GHz)	Gain(dB)	Ease of the fabrication
[31]	slotted bow tie with AMC & metamaterial lens (planar)	0.35 - 0.77	6.5	Complex
[32]	cavity backed CPW fed bowtie (planar)	0.36 - 0.55	6.68	Simple and low cost
This works	**Slot-backed CPW fed bowtie (planar)**	**2.26 -2.50**	**20**	**Simple and low cost**

5. CONCLUSION

In this paper, we design and fabricate a bowtie antenna for Ground Penetrating Radar (GPR) operating at 2.4 GHz. The antenna design and simulation were conducted using CST Microwave Studio. The simulation results demonstrated a good bandwidth, with a simulated bandwidth covering from 2.29 GHz to 2.50 GHz (BW = 210 MHz) and a minimal return loss at 2.4 GHz with S11 = (-25.49 dB). The measurement results indicate a return loss value of -18 dB at 2.42 GHz. The arc antenna achieved a maximum gain of 20 dB at the center frequency of 2.4 GHz, making it a suitable choice for GPR applications that require a higher antenna gain to penetrate deeper into the ground. Results shown demonstrated good agreement between the measured and simulated findings, as well as reliable, high-gain, and stable omnidirectional radiation characteristics in the targeted frequency regions. These studies served to verify the design. Therefore, we recommend this antenna for GPR applications. Future work should focus on the practical measurement and testing of the proposed antenna in GPR applications.

REFERENCES

[1] C. Way Chang, C. Hua Lin, and Q.-W. Yuan, "Quantitative study of electromagnetic wave characteristic values for mortar's crack," *Constr. Build. Mater.*, vol. 175, pp. 351–359, Jun. 2018, doi: 10.1016/j.conbuildmat.2017.09.171.

[2] K. Zajícová and T. Chuman, "Application of ground penetrating radar methods in soil studies: A review," *Geoderma*, vol. 343, pp. 116–129, Jun. 2019, doi: 10.1016/j.geoderma.2019.02.024.

[3] G. Alsharahi *et al.*, "Analysis and Modeling of GPR Signals to Detect Cavities: Case Studies in Morocco," *J. Electromagn. Eng. Sci.*, vol. 19, pp. 177–187, Jul. 2019, doi: 10.26866/jees.2019.19.3.177.

[4] G. Alsharahi, A. Driouach, and A. Faize, "Performance of GPR Influenced by Electrical Conductivity and Dielectric Constant," *Procedia Technol.*, vol. 22, pp. 570–575, Dec. 2016, doi: 10.1016/j.protcy.2016.01.118.

[5] O. Ismail, L. Youssef, O. Otman, and A. Aghanim, "Design of a Circular Patch Antenna with a reflector for GPR applications," *ITM Web Conf.*, vol. 48, p. 01004, 2022, doi: 10.1051/itmconf/20224801004.

[6] A. Raza, W. Lin, M. K. Ishfaq, M. Inam, F. Masud, and M. H. Dahri, "A Wideband Reflector-Backed Antenna for Applications in GPR," *Int. J. Antennas Propag.*, vol. 2021, p. e3531019, Nov. 2021, doi: 10.1155/2021/3531019.

[7] J. van der Kruk, N. Diamanti, A. Giannopoulos, and H. Vereecken, "Inversion of dispersive GPR pulse propagation in waveguides with heterogeneities and rough and dipping interfaces," *J. Appl. Geophys.*, vol. 81, pp. 88–96, Jun. 2012, doi: 10.1016/j.jappgeo.2011.09.013.

[8] A. Benedetto, F. Tosti, L. B. Ciampoli, and F. D'Amico, "GPR Applications Across Engineering and Geosciences Disciplines in Italy: A Review," *IEEE J. Sel. Top. Appl. Earth Obs. Remote Sens.*, vol. 9, no. 7, pp. 2952–2965, Jul. 2016, doi: 10.1109/JSTARS.2016.2554106.

[9] A. Chaabane and M. Guerroui, "Printed UWB Rhombus Shaped Antenna for GPR Applications," *Iran. J. Electr. Electron. Eng.*, vol. 17, no. 4, pp. 2041–2041, Dec. 2021, doi: 10.22068/IJEEE.17.4.2041.

[10] D. Aissaoui, A. Chaabane, A. Boualleg, and M. Guerroui, "Coplanar Waveguide-fed UWB Slotted Antenna with Notched-band Performance," *Period. Polytech. Electr. Eng. Comput. Sci.*, vol. 65, no. 1, Art. no. 1, Jan. 2021, doi: 10.3311/PPee.15869.

[11] A. E. Fatimi, S. Bri, and A. Saadi, "UWB antenna with circular patch for early breast cancer detection," *TELKOMNIKA Telecommun. Comput. Electron. Control*, vol. 17, no. 5, Art. no. 5, Oct. 2019, doi: 10.12928/telkomnika.v17i5.12757.

[12] J. Ali, N. Abdullah, M. Ismail, E. Mohd, and S. M. Shah, "Ultra-Wideband Antenna Design for GPR Applications: A Review," *Int. J. Adv. Comput. Sci. Appl.*, vol. 8, pp. 392–400, Aug. 2017, doi: 10.14569/IJACSA.2017.080753.

[13] M. Roslee, K. S. Subari, and I. S. Shahdan, "Design of bow tie antenna in CST studio suite below 2GHz for ground penetrating radar applications," in *2011 IEEE International RF & Microwave Conference*, Dec. 2011, pp. 430–433. doi: 10.1109/RFM.2011.6168783.

[14] C. Sibo, L. Jun, W. Tianhao, and Z. Yang, "Design of a drop-shaped ultra-wideband ground-penetrating radar antenna," in *2019 14th IEEE International Conference on Electronic Measurement & Instruments (ICEMI)*, Nov. 2019, pp. 145–149. doi: 10.1109/ICEMI46757.2019.9101874.

[15] A. Raza, W. Lin, Y. Chen, Z. Yanting, H. T. Chattha, and A. B. Sharif, "Wideband tapered slot antenna for applications in ground penetrating radar," *Microw. Opt. Technol. Lett.*, vol. 62, no. 7, pp. 2562–2568, 2020, doi: 10.1002/mop.32338.

[16] J. Colaco and J. Cotta, "Design, fabrication and performance analysis of floodlight shaped microstrip antenna for Wi-Fi/IoT applications," *Indones. J. Electr. Eng. Comput. Sci.*, vol. 27, p. 1462, Sep. 2022, doi: 10.11591/ijeecs.v27.i3.pp1462-1469.

[17] S. Palanivel Rajan and C. Vivek, "Analysis and Design of Microstrip Patch Antenna for Radar Communication," *J. Electr. Eng. Technol.*, vol. 14, no. 2, pp. 923–929, Mar. 2019, doi: 10.1007/s42835-018-00072-y.

[18] H. Indhuja Nivetha, T. Sathiyapriya, V. Gurunathan, A. Monasri, S. Sathish Kumar, and V. Selvaraj, "Design of High Gain Compact Microstrip Patch Antenna at ISM Band," 2023, Accessed: Dec. 17, 2023. [Online]. Available: https://essuir.sumdu.edu.ua/handle/123456789/92910

[19] A. Khabba *et al.*, "A new miniaturized wideband self-isolated two-port MIMO antenna for 5G millimeter-wave applications," *TELKOMNIKA Telecommun. Comput. Electron. Control*, vol. 21, no. 3, Art. no. 3, Feb. 2023, doi: 10.12928/telkomnika.v21i3.24139.

[20] M. Abri, H. Badaoui, and Z. Berber, "A Bow-Tie Bluetooth/Wimax Antenna Design for Wireless Networks Applications," *Int. J. Inf. Netw. Secur. IJINS*, vol. 1, Jul. 2012, doi: 10.11591/ijins.v1i3.733.

[21] S. Liu, M. Li, H. Li, L. Yang, and X. Shi, "Cavity-backed bow-tie antenna with dielectric loading for ground-penetrating radar application," *IET Microw. Antennas Propag.*, vol. 14, no. 2, pp. 153–157, 2020, doi: 10.1049/iet-map.2019.0309.

[22] N. Barkataki, B. Tiru, and U. Sarma, "A CNN model for predicting size of buried objects from GPR B-Scans," *J. Appl. Geophys.*, vol. 200, p. 104620, May 2022, doi: 10.1016/j.jappgeo.2022.104620.

[23] M. S. Rana, B. K. Sen, M. Tanjil-Al Mamun, M. S. Mahmud, and M. M. Rahman, "A 2.45 GHz microstrip patch antenna design, simulation, and analysis for wireless applications," *Bull. Electr. Eng. Inform.*, vol. 12, no. 4, pp. 2173–2184, 2023.

[24] N. Jaglan, S. D. Gupta, and S. Srivastava, "Notched UWB Circular Monopole Antenna Design Using Uni-Planar EBG Structures," *Int. J. Commun. Antenna Propag. IRECAP*, vol. 6, no. 5, Art. no. 5, Oct. 2016, doi: 10.15866/irecap.v6i5.9456.

[25] Y. Rahayu and I. Artiyah, "Design and Development of Microstrip Antenna Circular Patch Array for Maritime Radar Applications," *Sci. Technol. Commun. J.*, vol. 1, no. 3, Art. no. 3, Jun. 2021, doi: 10.59190/stc.v1i3.193.

[26] S. Chatterjee, A. Bhattacharya, and S. Duggal, "Methodology for utilization of a generalised antenna in gprMax simulator," in *Multimodal Sensing: Technologies and Applications*, SPIE, Jun. 2019, pp. 162–172. doi: 10.1117/12.2525520.
[27] H. N. Awl *et al.*, "Bandwidth improvement in bow-tie microstrip antennas: The effect of substrate type and design dimensions," *Appl. Sci.*, vol. 10, no. 2, p. 504, 2020.
[28] N. Barkataki, B. Tiru, and U. Sarma, "Performance investigation of patch and bow-tie antennas for ground penetrating radar applications," *Int. J. Adv. Technol. Eng. Explor.*, vol. 8, no. 79, pp. 753–765, 2021.
[29] M. Moulay and M. Abri, "Bowtie Antennas Design for Bluetooth/Wimax/Wifi Applications," *Int. J. Microw. Opt. Technol.*, vol. 9, no. 4, 2014.
[30] A. Mehadji, H. Badaoui, and Z. Berber, "A bow-tie Bluetooth/Wimax antenna design for wireless networks applications," *Int. J. Inf. Netw. Secur.*, vol. 1, no. 3, p. 207, 2012.
[31] Y. Li and J. Chen, "Design of Miniaturized High Gain Bow-Tie Antenna," *IEEE Trans. Antennas Propag.*, vol. 70, pp. 738–743, Jan. 2022, doi: 10.1109/TAP.2021.3098595.
[32] N. Barkataki, P. Borah, U. Sarma, and B. Tiru, "Design of a 400 MHz Cavity Backed CPW Fed Bow-Tie Antenna for GPR Applications," in *2021 International Conference on Industrial Electronics Research and Applications (ICIERA)*, Dec. 2021, pp. 1–6. doi: 10.1109/ICIERA53202.2021.9726755.